Nanotemplating of Calcium Phosphate Using a Double-Hydrophilic Block Copolymer

Wiliana Tjandra,[†] Jia Yao,[†,‡] Palaniswamy Ravi,[†] Kam C. Tam,*[,†] and Airin Alamsjah[†]

Singapore−MIT Alliance, School of Mechanical and Aerospace Engineering, Nanyang Technological University, 50 Nanyang Avenue, Singapore 639798, and Department of Chemistry, Zhejiang University, Hangzhou, People's Repubic of China 310027

Received March 30, 2005. Revised Manuscript Received June 23, 2005

Atom transfer radical polymerization technique was used to synthesize poly(ethylene oxide)-*block*-poly(methacrylic acid) (PEO-*b*-PMAA) copolymer, which was employed as a template for the controlled precipitation of calcium phosphate from aqueous solution at different pH values. The interactions between polymer and inorganic ions were studied using Ca^{2+} ion selective electrode, which indicated a possible weak interaction between Ca^{2+} and PEO segments, in addition to the interaction between Ca^{2+} and MAA segments. Two interesting superstructures consisting of an organized inorganic/organic hybrid material were characterized by electron microscopy. At pH ∼4.0 a nested structure consisting of hybrid nanofilaments was obtained. The fibers originate from a core of a size similar to that of the primary polymer aggregates, suggesting that cooperative interactions at a local level between dissolving calcium phosphate clusters and disassembling polymer segments may be responsible for the highly anisotropic character of the secondary growth process. At pH ∼9.0 fractal growth morphology was obtained through the mineralization process. Such calcium phosphate/polymer nanohybrids with complex morphologies are interesting and might also be useful as novel ceramic precursors, reinforcing fillers, or biomedical implants.

Introduction

It is self-evident that the organization and transformation of matter and energy are fundamental aspects of the universe. Although many approaches seek to mimic the information processing and sensing capabilities of biological nanostructures, they often lack the inherent materials-building properties typical of organisms, which are essential if nanostructures are to be organized across many length scales and used as functional materials within an integrated system.[1] Nanochemistry aims to extend the traditional length scales of synthetic chemistry and exploit the collective properties of organized assemblies produced by processes such as controlled crystallization and supramolecular complementarity. Morphosynthesis, the control of architecture and morphology and the patterning of inorganic materials with nanoscopic to macroscopic dimensions, has rapidly developed into a promising field in nanochemistry.[2] For example, chemical fabrication and microfabrication methods can be combined to produce externally patterned materials, whereas spontaneous processes associated with solvent evaporation, molecular cross-linking, or programmed recognition have been used to control the deposition of nanoparticle-based superlattices.[3]

Recently it was shown that the so-called double-hydrophilic block copolymers (DHBC) with appropriate molecular architecture could exert a strong influence on the external morphology and crystalline structure of inorganic colloids.[4] The underlying philosophy in this work is to use block copolymers comprised of one hydrophilic block designed to interact with selected inorganic salts and surfaces, and another hydrophilic block that promotes dissolution in water without strongly interacting with the inorganic precipitate or soluble precursors. Owing to the separation of the binding moiety on one side of the macromolecule and the solvating, noninteractive moiety on the other, complex patterns can be established, where both the binding and dispersive functions of the polymeric template are operational in the interacting or loaded state. Double-hydrophilic block copolymers were found to be extremely effective in the crystallization control of calcium carbonate, calcium phosphate, barium sulfate, barium chromate, and cadmium tungstate.[5]

As an extension of our early work on surfactant templating technique for the synthesis of nanoporous hydroxyapatite (HA),[6] block copolymer was used to synthesize polymer−

* Corresponding author. E-mail: mkctam@ntu.edu.sg.
[†] Nanyang Technological University.
[‡] Zhejiang University.

(1) Colfen, H.; Mann, S. *Angew. Chem., Int. Ed.* **2003**, *42*, 2350.
(2) (a) Archibald, D. D.; Mann, S. *Nature* **1993**, *364*, 430. (b) Mann, S.; Ozin, G. A. *Nature* **1996**, *382*, 313. (c) Li, M.; Schnablegger, H.; Mann, S. *Nature* **1999**, *402*, 393. (d) Estroff, L. A.; Hamilton, A. D. *Chem. Mater.* **2001**, *13*, 3227.
(3) (a) Yang, P.; Rizvi, A. H.; Messer, B.; Chmelka, B. F.; Whitesides, G. M.; Stucky, G. D. *Adv. Mater.* **2001**, *13*, 427. (b) Shenton, W.; Pum, D.; Sleytr, U. B.; Mann, S. *Nature* **1997**, *389*, 585. (c) Murray, C. B.; Kagan, C. R.; Bawendi, M. G. *Science* **1995**, *270*, 1335. (d) Wang, Z. L. *Adv. Mater.* **1998**, *10*, 13. (e) Andres, R. P.; Bielefeld, J. D.; Henderson, J. I.; Janes, D. B.; Kolagunta, V. R.; Kubiak, C. P.; Mahoney, W. J.; Osifchin, R. G. *Science* **1996**, *273*, 1690. (f) Galow, T. H.; Boal, A. K. V.; Rotello, M. *Adv. Mater.* **2000**, *12*, 576. (g) Mirkin, C. A.; Letsinger, R. L.; Mucic, R. C.; Storhoff, J. J. *Nature* **1996**, *382*, 607. (h) Mann, S.; Shenton, W.; Li, M.; Connolly, S.; Fitzmaurice, D. *Adv. Mater.* **2000**, *12*, 147. (i) Dujardin, E.; Hsin, L.-B.; Wang, C. R. C.; Mann, S. *Chem. Commun.* **2001**, 1264.
(4) (a) Colfen, H. *Macromol. Rapid Commun.* **2001**, *22*, 219. (b) Sedlak, M.; Antonietti, M.; Colfen, H. *Macromol. Chem. Phys.* **1998**, *199*, 247.

10.1021/cm050679b CCC: $30.25
Published on Web 08/20/2005

HA hybrids. In this paper, the atom transfer radical polymerization technique[7] was used to synthesize the poly(ethylene oxide)-*block*-poly(methacrylic acid) (PEO-*b*-PMAA) copolymer, and the polymer was employed as a dispersed template for the controlled precipitation of calcium phosphate from aqueous solution at different pH values. Some of the potential uses[8b] of these types of hybrids are novel ceramic precursors, which serve to form high-performance ceramic with reinforcing fillers to improve strength and density, in which the polymer directly mediates the compatibility of the matrix, or biomedical implants such as dental and bone implants.

Experimental Section

Materials. $CaCl_2$ and K_2HPO_4, were purchased from Aldrich and used without further purification. The monohydroxy capped poly(ethylene oxide) with a degree of polymerization of 44 (M_n = 1950 Da, by NMR) was donated by Dow Chemicals, Singapore. *tert*-Butyl methacrylate (*t*-BMA, 98% Aldrich) was passed through a basic alumina column, stirred over CaH_2, and distilled under reduced pressure. CuCl (99.995%,), *N*,*N*,*N*′,*N*′,*N*″,*N*″-hexamethyltriethylenetetramine (HMTETA, 98%), 2-bromoisobutryl bromide, and anisole were purchased from Aldrich and used without further purification.

Calcium Phosphate Mineralization in the Presence of Block Copolymers. *Preparation of Polymer Solution.* The polymer solutions were prepared by dissolving 0.1 g of polymer in 100 mL of deionized water and sonicated for 5 min, and filtered through a 0.45 μm membrane filter. Under these conditions, the PEO-*b*-PMAA copolymer dissolved in water to give a pH of 3.3 due to the weak carboxylic acid functionalities. The amount of carboxylic acid groups was calculated from titrating 1 M NaOH into the polymer solution. From the titration curves of pH and conductivity, we found that the carboxylic acid groups are fully neutralized to carboxylate groups at a pH greater than 9.

PEO-b-PMAA with calcium chloride. At pH 9, a known amount of PEO-*b*-PMAA solutions was neutralized by titrating with 100 mM $CaCl_2$ solution to obtain the desired values of degree of neutralization (DN) under stirring with a magnetic stirrer for 1 min, where DN is defined as

$$\mathrm{DN}\ (\%) = \frac{n_{Ca^{2+}}}{n_{COO^-}} \times 100 \qquad (1)$$

where $n_{Ca^{2+}}$ and n_{COO^-} are the moles of added Ca^{2+} ions and COO^- groups, respectively.

PEO-b-PMAA with Calcium Phosphate. Precipitation of calcium by the addition of phosphate was performed at three different initial pH values (4, 7, and 9) for the solution containing Ca^{2+} ions. In each case, stoichiometric amounts of phosphate in water (200 mM) were added to yield a Ca:P ratio of 1.67:1. The final pH was maintained at the initial value by the addition of NaOH or HCl, depending on the desired pH.

Physical Characterization Methods. Dynamic light scattering (DLS), surface tension titration (SFT), potentiometric titration measuring electromotive force (emf) using a calcium ion selective electrode (ISE), turbidimetry, wide-angle X-ray scattering (WAXS), transmission electron microscopy (TEM), and scanning electron microscopy (SEM) were employed to study the aggregation behavior of PEO-*b*-PMAA and calcium system, and the morphology of mineralization products.

Dynamic Light Scattering (DLS). DLS represents one of the more reliable techniques for studying the configuration and microstructure of polymeric micellar systems. The laser light scattering experiments were conducted using a Brookhaven laser light scattering system. This system consists of a BI200SM goniometer, BI-9000AT digital correlator, and other supporting data acquisition and analysis software and accessories. An argon ion vertically polarized 488 nm laser was used as the light source. The $G_2(t)$ functions obtained from DLS were analyzed using the inverse Laplace transformation technique (REPES in our case) to produce the distribution function of decay times. The concentration of the filtered polymer solutions (using 0.45 μm filter) investigated by light scattering is 0.01−0.1 wt %, which is in the dilute solution regime where the behavior of individual particles can be characterized. From dynamic light scattering, the hydrodynamic radii (R_h) of micelles were obtained.

Surface Tension Titration (SFT). The tensiometer Data Physics DCAT 21 system was employed to perform the surface tension titration.

Turbidimetry. The turbidity was measured with an Agilent 8453 UV−visible spectroscopy system. The turbidity was calculated from the expression (100 − *T*)/100, where *T* is the transmittance (%) at 650 nm.

Potentiometric Titration. The interactions between PEO-*b*-PMAA and Ca^{2+} were investigated using the electromotive (emf) technique coupled with a Ca^{2+} ion selective electrode (Ca^{2+} ISE) and a reference Ag/AgCl electrode. The titration experiments were conducted using the Radiometer Copenhagen ABU93 Triburette system. Titration of $CaCl_2$ solution into water was measured to calibrate the electrode; the Nernst equation is emf = 77.071 + 23.778 log $C_{Ca^{2+}}$, which was used to calculate the mobile Ca^{2+} ion concentration through the emf value.

Wide-Angle X-ray Scattering (WAXS). STD-XRD was performed using a standard attachment XRD 6000 Shimadzu with Cu Kα tube operated at 50 kV and 20 mA. XRD was performed on centrifuged and dried samples.

Transmission Electron Microscopy (TEM). TEM was performed on a JEOL JEM-2010 electron microscope at an acceleration voltage of 200 kV. A copper grid (400 mesh) with a carbon film was used. The copper grid was immersed in a drop of the aqueous sample solution, and dried overnight at room temperature prior to measurement. Energy-dispersive X-ray microanalysis (EDX) was done using Link ISIS from Oxford, which is attached to the TEM.

Scanning Electron Microscopy (SEM). SEM was carried out with a Leica S360 scanning electron microscope. The samples were prepared by evaporating a drop of the sample solutions on a glass plate, and gold was coated on the sample surface with 80 s sputtering time, 2 mbar pressure, and 18 mA current.

Results and Discussion

Microstructure of PEO-*b*-PMAA in Calcium Chloride Solutions. The synthesis of PEO-*b*-PMAA was carried out

(5) (a) Colfen, H.; Antonietti, M. *Langmuir* **1998**, *14*, 582. (b) Qi, L.; Colfen, H.; Antonietti, M. *Angew. Chem., Int. Ed.* **2000**, *39*, 604. (c) Qi, L.; Colfen, H.; Antonietti, M.; Li, M.; Hopwood, J. D.; Ashley, A. J.; Mann, S. *Chem.*—Eur. J. **2001**, *7*, 3526. (d) Yu, S. H.; Colfen, H.; Antonietti, M. *Chem.*—Eur. J. **2002**, *8*, 2937. (e) Yu, S. H.; Antonietti, M.; Colfen, H.; Giersig, M. *Angew. Chem., Int. Ed.* **2002**, *41*, 2356. (f) Yu, S. H.; Antonietti, M.; Colfen, H.; Hartmann, J. *Nano Lett.* **2003**, *3*, 379.
(6) Yao, J.; Tjandra, W.; Chen, Y. Z.; Tam, K. C.; Ma, J.; Soh, B. *J. Mater. Chem.* **2003**, *13*, 3053.
(7) (a) Ravi, P.; Wang, C.; Tam, K. C.; Gan, L. H. *Macromolecules* **2003**, *36*, 173. (b) Yao, J.; Ravi, P.; Tam, K. C.; Gan, L. H. *Langmuir* **2004**, *20*, 2157. (c) Matyjaszewski, K.; Xia, J. *Chem. Rev.* **2001**, *101*, 2921.
(8) (a) Solomatin, S.; Bronich, T.; Eisenberg, A.; Kabanov, V. A.; Kabanov, A. V. *Langmuir* **2004**, *20*, 2066−2068. (b) Antonietti, M.; Breulmann, M.; Goltner, C.; Colfen, H.; Wong, K. K.; Walsh, D.; Mann, S. *Chem.*—Eur. J. **1998**, *4*, 2493.

Scheme 1. Synthesis of PEO-*b*-PMAA

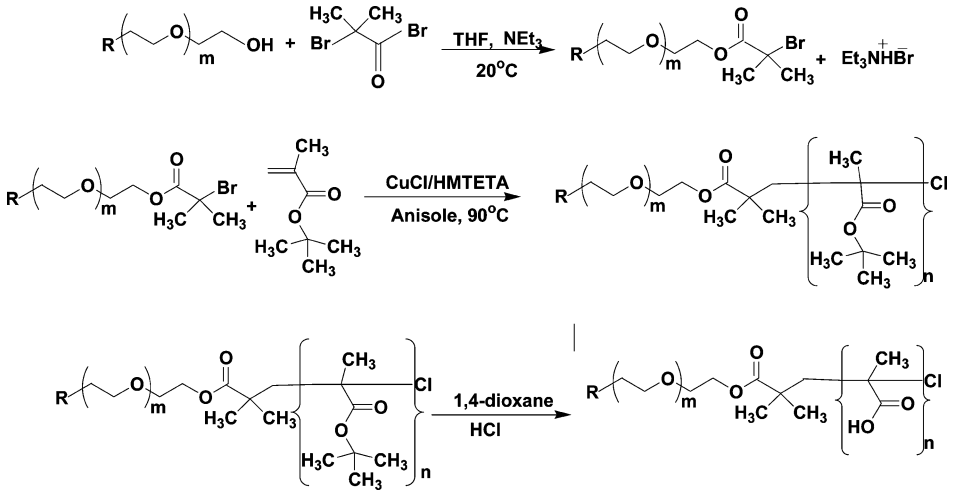

using the atom transfer radical polymerization (ATRP) technique (Scheme 1). The detailed ATRP technique for the synthesis of PEO-*b*-PMAA is described in the Supporting Information.

PEO-*b*-PMAA can form aggregates through the hydrophobic induced hypercoiling of PMAA segments at low pH. The particle size R_h is about 35 nm at pH 3, and the micelles disintegrate into unimers when the pH exceeds 5, when the COOH groups are ionized to COO^- groups.

When Ca^{2+} ions are introduced into PEO-*b*-PMAA solutions at high pH, the PMAA block becomes neutralized by metal ions, which leads to the formation of aggregates, where the alkali earth metal ions are simply bound to PMAA segments via electrostatic interaction, forming an insoluble hydrophobic core that is stabilized by a PEO corona. To determine the effects of Ca^{2+} concentration on the aggregation behavior, we performed titrations of $CaCl_2$ into PEO-*b*-PMAA solutions at pH 9, 7, and 4 (degree of ionization (α) = 1, 0.5, and 0, respectively) and the surface tension, particle size, turbidity, and mobile Ca^{2+} concentration were measured.

Figure 1a shows the surface tension curve, where 100 mM $CaCl_2$ solution was titrated into PEO-*b*-PMAA solution at pH 9 (COO^- concentration was 5.3 mM, which was calculated from the titration of NaOH into the PEO-*b*-PMAA solution). On the basis of the changes in the slope, we can divide the curve into four regimes.

In the first region, the surface tension decreases rapidly, which means the PMAA segments become more hydrophobic as Ca^{2+} ions are bonded to COO^- groups. Since the amphiphilic polymeric chains induced by the complexation with Ca^{2+} ions will partition to the air/water interface, the surface tension exhibits a sharp decrease. In region 2, further titration of Ca^{2+} ions leads to the formation of micelles induced by the complexation of Ca^{2+} with PMAA segments, which depletes the concentration of polymer chains at the air−water interface. Thus, the reduction in the surface tension as depicted by the slope in region 2 is much lower than in region 1. We observed an inflection point at DN = 25% for the transition from region 1 to region 2 representing a charge ratio of 0.5 (ratio of moles of Ca^{2+} to COO^-) on the polymer chains. At this condition, the repulsion between PMAA segments is significantly reduced, and the hydrophobicity of PMAA/Ca^{2+} complex induces the micellization of simplex micelles. The changes in the particle size in regions 1 and 2 were measured by DLS to determine the R_h at DN of 20 and 40%. We found no aggregates at DN of 20%; however, particles with R_h of about 21.5 nm were observed at DN of 40%, which is consistent with the simple core−shell micelle comprised of a PMAA/Ca^{2+} core and a PEO shell.

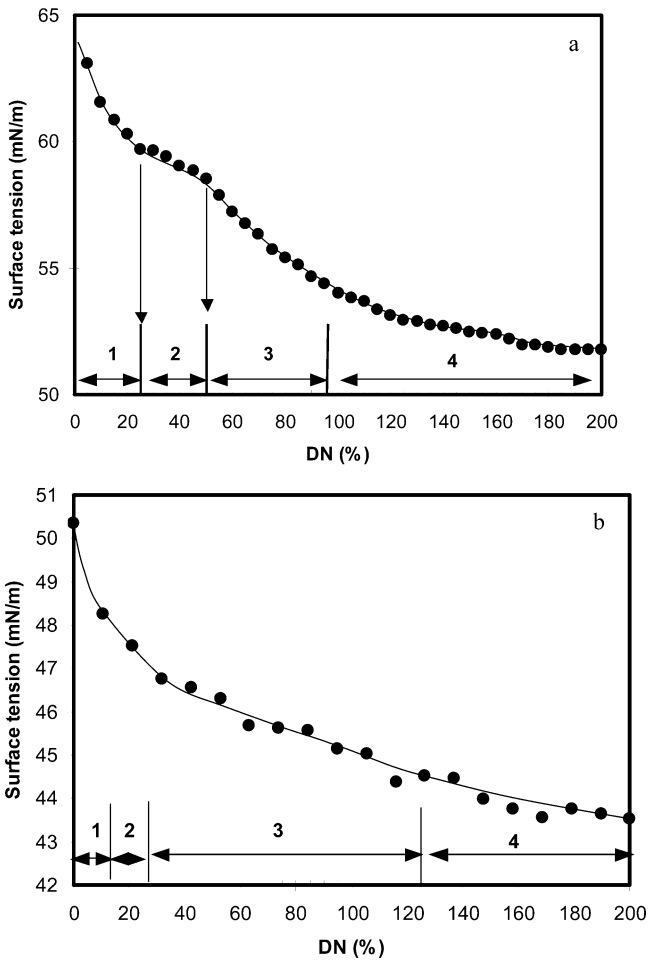

Figure 1. (a) Surface tension curve for titration of $CaCl_2$ into solution containing PEO-*b*-PMAA at pH 9. (b) Surface tension curve for titration of $CaCl_2$ into solution containing PEO-*b*-PMAA at pH 7.

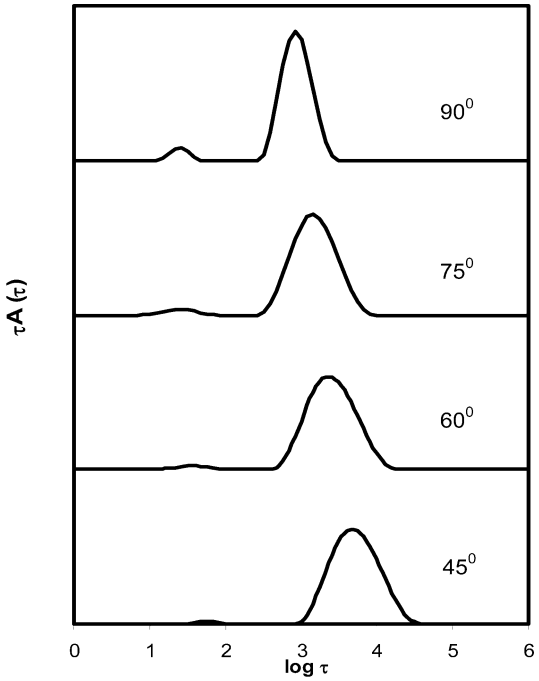

Figure 2. Angle dependence of relaxation time distribution functions for PEO-*b*-PMAA at pH 9 in 100% DN of Ca^{2+} ions.

Region 2 extends to DN of 50%, where the COO^- groups on PMAA segments are fully neutralized by Ca^{2+}. Increasing amounts of Ca^{2+} ions will lead to a decrease in the surface tension, and this is probably caused by the interaction between PEO chains. As PMAAs are initially highly charged, there is a higher local concentration of Ca^{2+} around the polymer chains. Therefore, the excess Ca^{2+} perturbs the hydrogen bonds between PEO and water, which reduces the solubility of PEO chains. The combined effect of this and the minimization of electrostatic repulsion induced the formation of large aggregates. From DLS measurements, R_h at DN of 60 and 80% was found to be 50.3 and 65.5 nm, respectively. Region 4 represents the precipitation of the polymer/calcium complex at high Ca^{2+} ion concentration. The solution became cloudy at DN greater than 100%, which was also evident during the potentiometric titration experiments. Since the PEO-*b*-PMAA polymer contains 90 units of PMAA segments and 44 units of PEO segments, complexation of PMAA with Ca^{2+} will yield a reasonably hydrophobic PMAA−Ca^{2+} complex. As Ca^{2+} disturbs the hydrogen bonds of water and PEO chains, increasing the concentration of Ca^{2+} ions will dehydrate the PEO chains resulting in a lower solubility of PEO.

Figure 1b shows the surface tension measurement at pH 7 ($\alpha = 0.5$). Four regimes were observed, marked by changes in the slopes around DN of 12.5, 25, and 125%. The micelles start to form around DN of 12.5% and cease at DN of 25%, which is the theoretical limit when the ionized groups on PMAA are fully neutralized by Ca^{2+} (half the value compared to the condition at pH 9). As there are fewer charges on PMAA at pH 7 compared to pH 9, the local concentration of Ca^{2+} around the polymer chains is lower. Thus, the PEO blocks are sufficiently hydrophilic, and hence precipitation of the complex at a high DN was not observed. At pH 4 ($\alpha = 0$), all the carboxylic acid groups are not

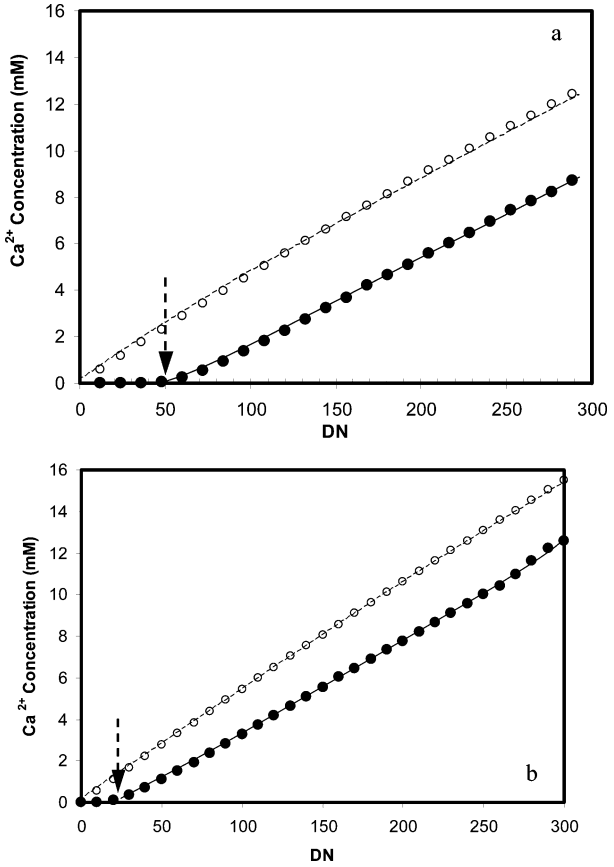

Figure 3. (a) Changes in Ca^{2+} ion concentration during the titration of $CaCl_2$ into solution of PEO-*b*-PMAA at pH 9. (●) Concentration of mobile Ca^{2+} ion; (○) total Ca^{2+} ions added. (b) Changes in Ca^{2+} ion concentration during titration of $CaCl_2$ into solution of PEO-*b*-PMAA at pH 7. (●) Concentration of mobile Ca^{2+} ion; (○) total Ca^{2+} ions added.

protonated (i.e., there are no COO^- groups present); hence no interaction between Ca^{2+} and the polymer is observed.

Figure 2 shows the relaxation time distributions at different scattering angles for the sample at pH 9 and DN of 100%. There are two relaxation modes in the distribution function: the slow mode represents the large aggregate with R_h of about 156 nm and the fast mode corresponds to a particle size of 2.2 nm, which is likely to be the polymeric chains.

Figure 3a shows the change in the concentration of mobile Ca^{2+} during the titration of $CaCl_2$ into PEO-*b*-PMAA solution at pH 9 ($\alpha = 1$). Additional Ca^{2+} ions up to DN of 50% results in the complete complexation of Ca^{2+} with COO^- groups on protonated PMAA blocks, as is evident by the absence of mobile Ca^{2+} ions over this concentration regime. When the DN exceeds 50%, the concentration of mobile Ca^{2+} ions increases linearly; its slope is slightly smaller than that for the titration of Ca^{2+} ions into polymer-free solution (○) of similar ionic strength. The difference between the experimental data and the solid line represents the amounts of Ca^{2+} bound to polymeric chains. Such a phenomenon is related to long-range electrostatic attraction of oppositely charged molecules resulting in the immobilization of Ca^{2+} ions, which is responsible for the disruption of hydrogen bonds between PEO chains and water.

Figure 3b shows the change in the concentration of mobile Ca^{2+} ions at pH 7 ($\alpha = 0.5$). We observed complete binding of Ca^{2+} ions for DN ranging from 0 to 25%, which is half

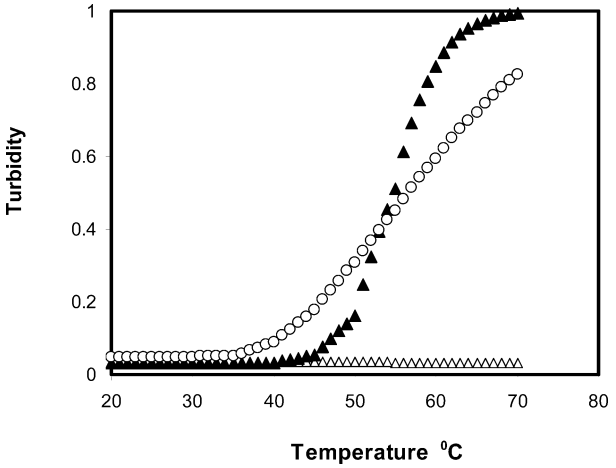

Figure 4. Turbidity measurements for (△) DN 40%, (▲) DN 100%, and (○) DN 300%.

the amounts observed when the solution was conditioned at pH 9. A similar difference in the slope between the solid line and the experimental data was observed. However, for the solution at pH 4, all the Ca^{2+} ions titrated to the polymer solution remained mobile.

The turbidity measurements at pH 9 were conducted to examine the effect of Ca^{2+} ions on the cloud point of the system, which is shown in Figure 4. We could not observe any cloud point at DN of 40%, as the solution remained clear during the temperature scan from 20 to 75 °C. As observed from light scattering measurements, we believe the clear solution constitutes a micellar complex consisting of PMAA/Ca^{2+} hydrophobic core stabilized by PEO corona, thereby yielding a stable micellar dispersion. At DN of 100%, we observed an obvious transition at 45 °C, which suggests that excess amounts of Ca^{2+} ions will result in the dehydration of PEO chains, making them hydrophobic and resulting in the lowering of the lower critical solution temperature (LCST) of PEO. This agrees with the literature where the addition of salt lowers the LCST.[8] With increasing temperatures, the hydrogen bonds between PEO chains and water are disrupted, which results in the dehydration of PEO chains that eventually leads to the precipitation of PEO segments from solution. As precipitation occurs at DN of 300%, the turbidity curve was measured by taking the solution at the clear upper region of the cuvette. The measured transition temperature of this solution is 35 °C, which is less than that at DN of 100%. This might indicate that it is easier to obtain a lower cloud point with a higher Ca^{2+} concentration.

The present study on PEO-*b*-PMAA in the presence of calcium chloride revealed interesting interactions between PEO-*b*-PMAA and Ca^{2+} ions. Since the PMAA block is longer than the PEO block (90 mol of MAA:44 mol of EO), the increase in the hydrophobicity from the PMAA/Ca^{2+} complex at high pH contributes to the reduced solubility of the system. At high pH, addition of $CaCl_2$ imparts amphiphilic character to the double-hydrophilic PEO-*b*-PMAA block copolymer. Micelles are induced when COO^- groups are fully complexed with Ca^{2+} ions, and at the same time excess Ca^{2+} ions dehydrate the PEO block, which induces the formation of secondary aggregates whose size increases

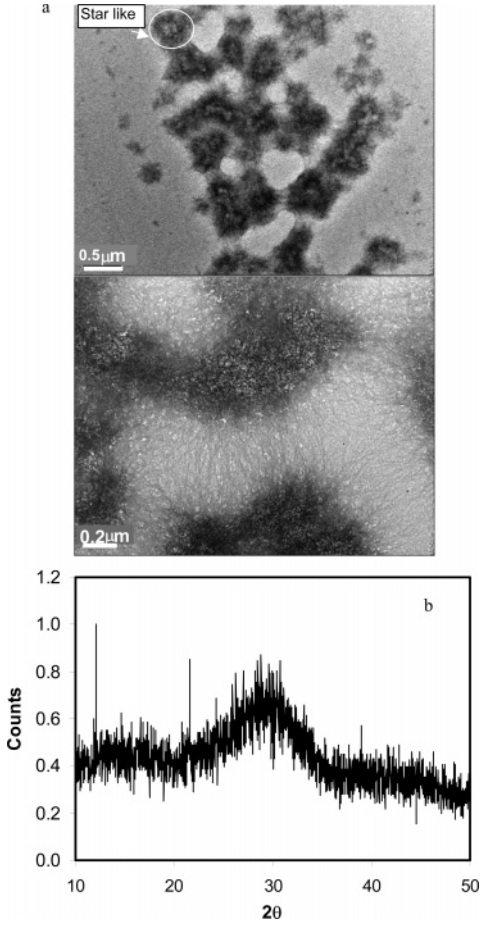

Figure 5. (a) TEM images showing calcium phosphate/polymer mesostructures at pH 4. (b) WAXS of the calcium phosphate/polymer at pH 4.

with $CaCl_2$ concentration until precipitation at DN of 100% and higher.

Interaction of PEO-*b*-PMAA with Calcium Phosphate. Precipitation of calcium by adding calcium phosphate was conducted at three different pH values (4, 7, and 9) for the Ca^{2+}-containing dispersion with DN of 300% at room temperature. In each case, stoichiometric amounts of phosphate in water (20 mM) were added to yield a Ca:P ratio of 1.67:1. The samples at different conditions were taken for observation under the TEM or SEM.

We observed interesting morphological forms for samples prepared at pH 4 as shown in Figure 5a. Under this condition, the hybrid consists of hairlike nanofilaments of approximately several nanometers in width. The filaments are usually associated with an electron-dense area of about 200 nm in thickness, although starlike shapes with no apparent entanglements at the core were also observed. We believe that the starlike particles represent the early stages in the development of the complex architecture, and with time, the filaments become interconnected to give extended neural network structures comprised of higher concentrations of hybrid structure. These complex structures represent higher order coupling of the cooperative growth processes and indicate that long-range organization can be established in this system. We also found that the morphology remains stable over a period of months. One possibility is that further growth process is suppressed by the relatively high solubility equilibrium of Ca^{2+} and phosphate ions at pH 4. At room

Scheme 2. Formation of Whiskers at pH 4

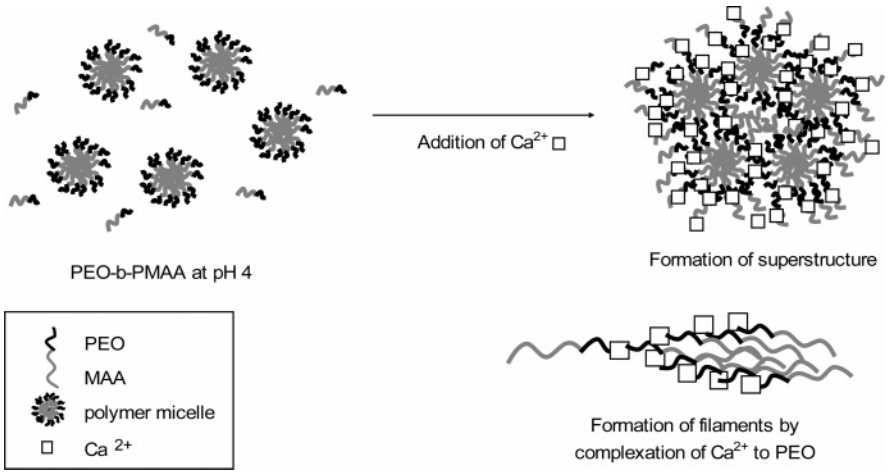

temperature and pH values of 2−6, dicalcium phosphate dihydrate (brushite) is preferentially formed; its solubility parameter is given by $-\log(K_{sp}) = 6.59$.[9] Wide-angle X-ray scattering (WAXS) was performed on centrifuged and dried samples as shown in Figure 5b, and the first two peaks (at $2\theta \sim 12°$ and 21°) suggest the presence of brushite. However, the wide lines suggest that the overall dried state is amorphous, which is caused by the presence of the polymer. This morphology also shows some similarity to that of colloidal calcium phosphate controlled by polyaspartates.[10] This superstructure is induced by DHBC acting as templates, since the control experiment done in the absence of polymer yields plateletlike brushite.

The above result is consistent with a previous study[8] on the templating process using PEO-*b*-PMAA-C_{12} containing three COOH groups, where the authors observed neuronlike structure. However, due to the short PMAA block, they only obtained polydispersed spheres. The micellization induced by hydrophobic C_{12} alkyl groups is believed to play an important role in the formation of the neuronlike structure. In our present study, we utilized longer PMAA segments, and we observed that micelles containing a swollen PMAA core are produced at a low pH of 4.

We proposed that Ca^{2+} ions are attracted to PEO chains of the polymeric micelles. As the hydrogen bond between PEO and water is disrupted by the complexation of Ca^{2+} ions and water, the micelles become more hydrophobic. As a result, the micelles form a "hollow starlike" structure to minimize the exposure of hydrophobic segments to water. It is possible that the entanglement of PEO chains of micelles and the complexation of calcium ions with unimeric PEO chains enable the growth of these filaments.

Figure 6 shows the evolution of the morphology at pH 9. We observed connecting spherical particles 2 days after phosphate was added to the sample. This is expected as the DHBC micelles are spherical with calcium phosphate located at the core. WAXS and energy-dispersive X-ray spectrometry (EDX) indicate the formation of amorphous calcium phosphate (ACP) at pH 9 and at Ca/P ratio of 1.56. As this is a hybrid structure, the amorphous polymeric chains disturb the overall crystallinity, as indicated by the WAXS spectra. After

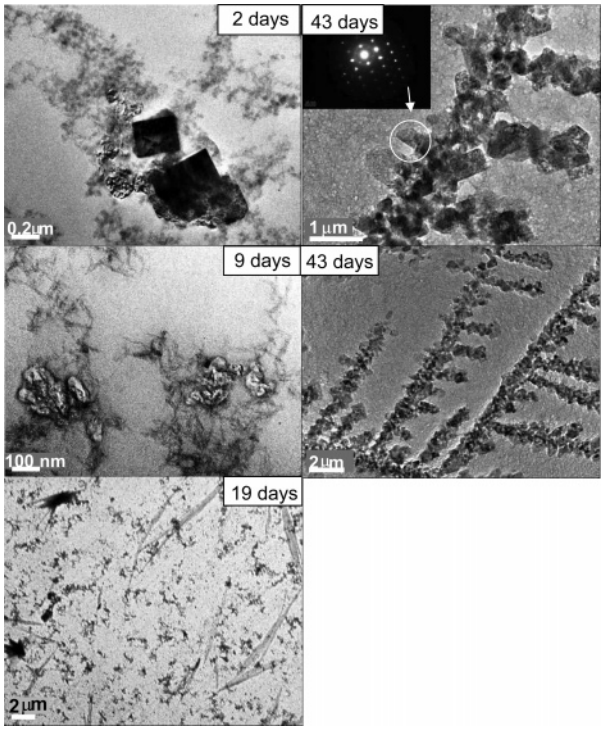

Figure 6. TEM images showing evolution of calcium phosphate/polymer mesostructures at pH 9.

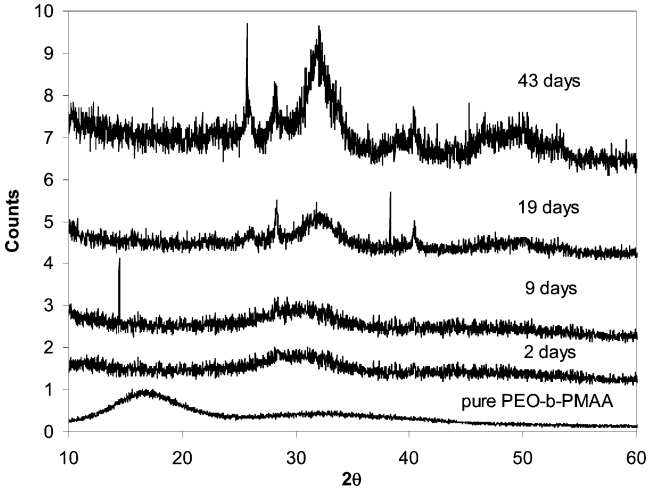

Figure 7. WAXS analysis on calcium phosphate hybrid at pH 9 in pure PEO-*b*-PMAA and polymer/calcium phosphate complex at 2, 9, 19, and 43 days.

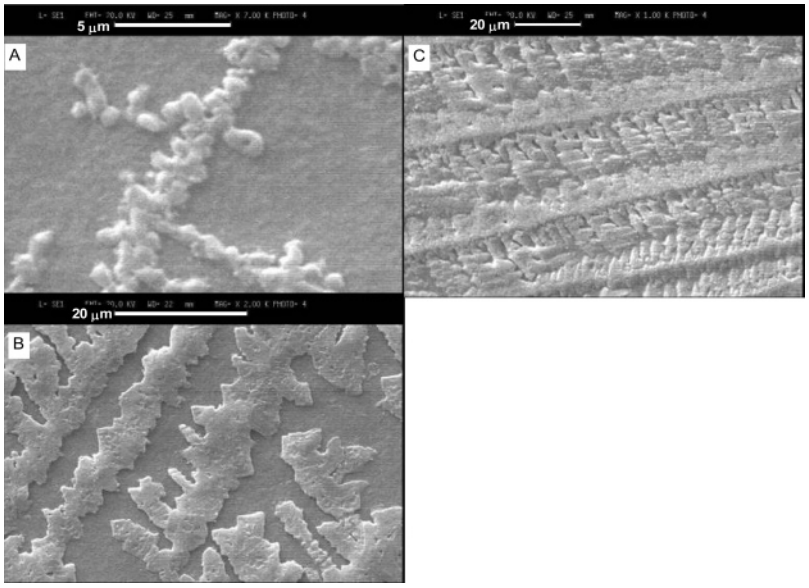

Figure 8. SEM images showing similar morphology of calcium phosphate/polymer mesostructures at pH 9.

Table 1. EDX during Morphogenesis of HA

time	Ca:P
day 2	1.56
day 9	1.62
day 19	1.65
day 43	1.67

incubation of the sample for 9 days, the spherical particles merged; this transition is caused by the growth of calcium phosphate due to diffusion of Ca^{2+} ions from micellar core, since the Ca/P ratio is now 1.62. The overall state of the calcium phosphate is ACP, as indicated from WAXS. Some denser cores are also produced, which may be caused by crystalline OCP, as suggested by the peak at 39°. However, as hydroxyapatite (HA) is more stable, slow diffusion of Ca^{2+} ions from the denser OCP cores led the dissimilation of the initial structure to form elongated HA crystals (several micrometers), as revealed by the TEM picture after 19 days. The entire needlelike morphology from day 9 has already reorganized to form isolated dense cores, which elongate over time. Such microstructural evolution is attributed to the crystallization of HA, as confirmed by WAXS and EDX. After 43 days, the sample shows a very interesting morphology. We observed treelike structures where the crystals of about 200 nm are aligned in a very ordered and organized manner. The crystals are believed to be NaCl crystals, which grow on smaller HA−polymeric hybrids, as revealed by WAXS and EDX results. The WAXS and EDX results are presented in Figure 7 and Table 1, respectively. Since the HA−polymer hybrids could be dispersed in solution through the hydrophilic PEO blocks, the equilibrium between the ions in solution with the hybrids can induce the growth of the crystals. The ordered alignment of crystals may be caused by affinity between the crystals during sample preparation, and the hydrophilic PEO blocks may also play an important role in producing the aligned morphology. The SEM pictures in Figure 8 were also measured at 43 days. The treelike structures in different regions of the sample were analyzed. Figure 8A shows the initial phase of alignment during the sample drying step, where the original particle shape can still be observed. Figure 8B reveals the morphology as moisture was progressively removed via evaporation, where the precipitation of salts grows on the backbone created by HA−polymeric hybrids. Figure 8C shows the morphology after the water was completely removed, and all the salt grows on the backbones to produce an ordered and aligned morphology. This contrasts with the control sample without DHBC. Figure 9 confirms the role of DHBC in the crystallization behavior of calcium phosphate. The morphological evolution at pH 7 was also examined, and spherical particles of 10−125 nm in size with a broad particle size distribution were observed.

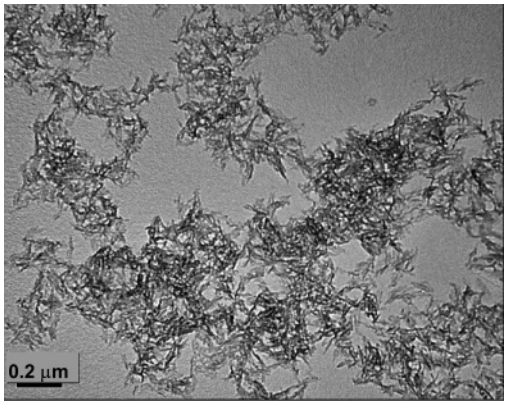

Figure 9. TEM image of calcium phosphate without DHBC at pH 9 after 43 days.

Conclusions

Our study on PEO-*b*-PMAA/calcium chloride system revealed interesting interactions between PEO-*b*-PMAA and Ca^{2+} ions. At high pH, addition of $CaCl_2$ imparts amphiphilic character to PEO-*b*-PMAA block copolymer, which induces micellar formation when the COO^- groups are fully complexed with Ca^{2+} ions. Excess Ca^{2+} ions dehydrate the PEO

(9) Epple, M.; Dorozhkin, S. V. *Angew. Chem., Int. Ed.* **2002**, *41*, 3130.
(10) Peytcheva, A.; Colfen, H.; Schnablegger, H.; Antonietti, M. *Colloid Polym. Sci.* **2002**, *280* (3), 218−227.

block and may induce the formation of secondary aggregates whose size increases with $CaCl_2$ concentration, which eventually leads to precipitation when DN exceeds 100%. Addition of phosphate to PEO-*b*-PMAA/calcium chloride solutions produces interesting structures. At pH 4, hybrids consisting of hairlike nanofilaments of several nanometers in width are produced. At pH 9, controlled crystallization was observed, where the diffusion of Ca^{2+} transformed the ACP into HA−polymer hybrids. We observed aligned treelike structures, which are interesting and might also be useful as novel ceramic precursors, reinforcing fillers, or biomedical implants.

Acknowledgment. J.Y. and P.R. wish to acknowledge financial support for the postdoctoral fellowship provided by the Singapore−MIT Alliance (SMA). W.T. acknowledges the Ph.D. scholarship provided by Nanyang Technological University.

Supporting Information Available: Synthetic procedure for block copolymer, PEO-*b*-PMAA; polymer characterization by GPC and NMR (PDF). This material is available free of charge via the Internet at http://pubs.acs.org.

CM050679B